SH2 domain containing leukocyte phosphoprotein of 76-kDa (SLP-76) feedback regulation of ZAP-70 microclustering

Hebin Liu[a], Marco A. Purbhoo[b], Daniel M. Davis[b], and Christopher E. Rudd[a,c,1]

[a]Cell Signalling Section, Department of Pathology, University of Cambridge, Cambridge CB2 1QP, United Kingdom; [b]Division of Cell and Molecular Biology, Imperial College London, London SW7 2AZ, United Kingdom; and [c]Cambridge Institute for Medical Research, Addenbrookes Hospital, Cambridge CB2 0XY, United Kingdom

Edited by Stuart F. Schlossman, Dana-Farber Cancer Institute, Boston, MA, and approved April 15, 2010 (received for review August 16, 2009)

T cell receptor (TCR) signaling involves CD4/CD8-p56lck recruitment of ZAP-70 to the TCR receptor, ZAP-70 phosphorylation of LAT that is followed by LAT recruitment of the GADS-SLP-76 complex. Back regulation of ZAP-70 by SLP-76 has not been documented. In this paper, we show that anti-CD3 induced ZAP-70 cluster formation is significantly reduced in the absence of SLP-76 (i.e., J14 cells) and in the presence of a mutant of SLP-76 (4KE) in Jurkat and primary T cells. Both the number of cells with clusters and the number of clusters per cell were reduced. This effect was not mediated by SLP-76 SH2 domain binding to ZAP-70 because SLP-76 failed to precipitate ZAP-70 and an inactivating SH2 domain mutation (i.e., R448L) on SLP-76 4KE did not reverse the inhibition of ZAP-70 clustering. Mutation of R448 on WT SLP-76 still supported ZAP-70 clustering. Intriguingly, by contrast, LAT clustering occurred normally in the absence of SLP-76, or the presence of 4KE SLP-76 indicating that this transmembrane adaptor can operate independently of ZAP-70-GADS-SLP-76. Our findings reconfigure the TCR signaling pathway by showing SLP-76 back-regulation of ZAP-70, an event that could ensure that signaling components are in balance for optimal T cell activation.

clustering | signaling | SLP-76 | T-cells | ZAP-70

T cell receptor (TCR) and CD4/CD8-p56lck ligation initiates a tyrosine phosphorylation cascade needed for T cell activation (1–3). p56lck phosphorylates the TCRζ and CD3 chains that recruit ZAP-70 leading to phosphorylation of adaptors such as linker for LAT (activation of T cells) and SLP-76 (SH2 domain containing leukocyte phosphoprotein of 76 kDa). LAT is a transmembrane adaptor with tyrosine residues that bind to the SH2 domains of Grb2-related adaptor downstream of Shc (GADS), growth factor receptor-bound protein 2 (Grb2) and phospholipase Cγ-1 (PLCγ1) (1, 4). GADS binds to LAT and recruits SLP-76 (SH2 domain containing leukocyte phosphoprotein of 76 kDa) by means of SH3 domain binding to a unique motif in SLP-76 (5). Each adaptor is needed for optimal thymic differentiation and activation of PLCγ1 (6–8). The SH2 domain of SLP-76 in turn binds to another adaptor ADAP (adhesion and degranulation promoting adapter protein) and the phosphatase hematopoietic progenitor kinase 1 (HPK1) via YDDV motifs (9–13). ADAP in turn binds to the *src* kinase-associated phosphoprotein 1 [(SKAP1) also *src* kinase-associated phosphoprotein-55 (SKAP-55)], an effecter of LFA-1 adhesion (14, 15).

The past decade has witnessed the introduction of powerful imaging techniques to T cell biology, showing that TCR ligation triggers the assembly of individual microclusters that mediate signaling (16–19). These signaling clusters of 200- to 500-nm-diameter form within seconds at the immunological synapse (IS) between a T cell and antigen presenting cells (APCs) (20–23). TCR clusters then coalesce to form the central supramolecular activation complex (SMAC) (24–26). A single TCR cluster can alter intracellular calcium levels (21–23). Although ZAP-70 are recruited into TCR clusters dependent on *src* kinases (22), peripheral SMAC formation requires SLP-76 binding to YDDV sites on ADAP (27). LAT, GADS, and SLP-76 clusters also transiently intersect TCR clusters (21, 22). ZAP-70 clusters are less motile than LAT and SLP-76 clusters that in turn disappear more rapidly from the contact area (21–23). Although the inhibitory coreceptor CTLA-4 potentially inhibits ZAP-70 cluster formation (28), whereas very late antigen 4 (VLA-4) can stabilize their presence (29).

The current model of the TCR pathway involves a linear sequence of events in which activated ZAP-70 phosphorylates LAT (and SLP-76), followed by LAT recruitment of GADS-SLP-76. The potential for reverse or feedback regulation of ZAP-70, GADS, and LAT clustering by SLP-76 has not been reported. Here, using imaging techniques, we demonstrate that SLP-76 exerts control over the clustering of ZAP-70, whereas LAT clustering operates distinct from cytoplasmic ZAP-70, GADS, and SLP-76.

Results

SLP-76 Is Essential for ZAP-70 Microcluster Formation. To assess whether ZAP-70 microcluster formation can be regulated by SLP-76, ZAP-70-mRFP was initially expressed in WT and SLP-76 deficient J14 Jurkat cells followed by imaging at the point of contact with immobilized anti-CD3 on slides, as previously reported (22, 23). ZAP-70-mRFP in WT cells underwent detectable clustering over a time-course of 0–80 s following contact with the surface of the anti-CD3–coated slide (Fig. 1*Ai Upper Right*, Fig. S1*A*, and Movie S1). Approximately 32% of cells showed newly formed clusters with an average of 18 clusters per positive cell over the time course (Fig. 1*A ii* and *iii*, gray bars). Slides coated with mock anti-Ig showed no clusters (Fig. 1*Ai Upper Left*). As previously reported (21, 23), ZAP-70-mRFP clusters underwent little movement as seen in tracking plots (Fig. S1*Ae*) and by the small displacement values (i.e., movement from the origin over time) that were objectively derived using Volocity software (Fig. 1*Aiv*). Motility also varied with the concentration of anti-CD3 where higher concentrations (i.e., greater strength of signal) generated larger and less motile clusters (Fig. S1*B a–f*). By contrast, J14 cells showed significantly reduced numbers of cells with ZAP-70-mRFP clusters (i.e., mean of 11 vs. 32% of cells) and reduced numbers of clusters per positive cell (i.e., mean of 9 vs. 18) (Fig. 1*A i Lower; ii* and *iii* red bars,). The same difference was detected at later times (i.e., 125–300 s). ZAP-70-

Author contributions: H.L., M.A.P., D.M.D., and C.R. designed research; H.L. and M.A.P. performed research; H.L. and C.R. wrote the paper; D.M.D. contributed new reagents/analytic tools; and D.M.D. and C.R. analyzed data.

The authors declare no conflict of interest.

This article is a PNAS Direct Submission.

Freely available online through the PNAS open access option.

[1]To whom correspondence should be addressed. E-mail: cer51@cam.ac.uk.

This article contains supporting information online at www.pnas.org/lookup/suppl/doi:10.1073/pnas.0909112107/-/DCSupplemental.

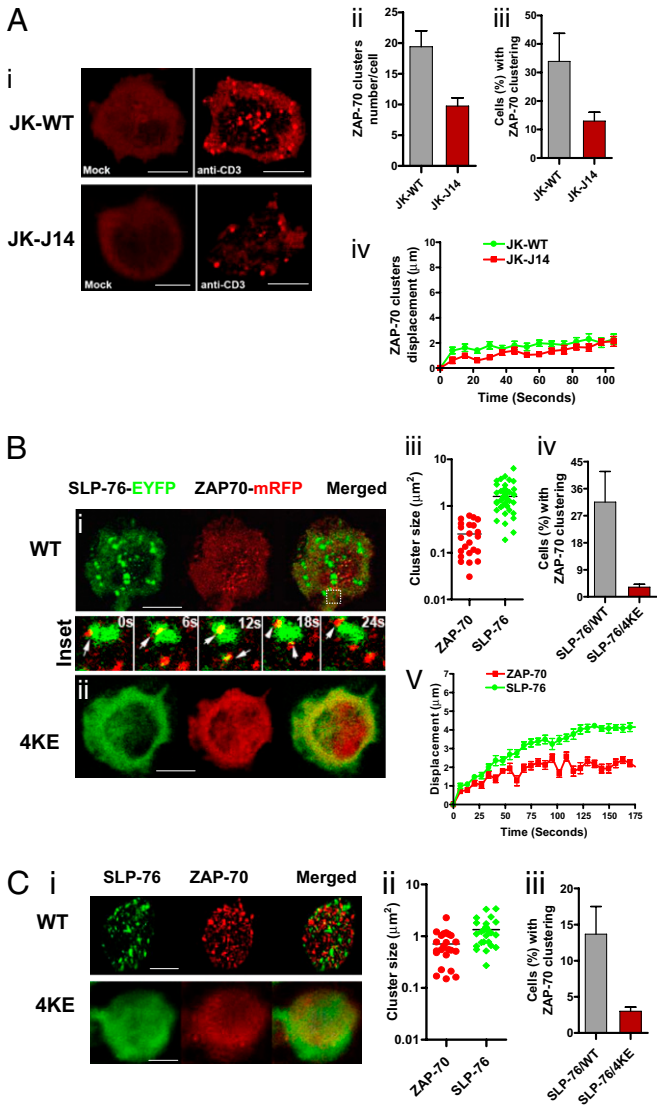

Fig. 1. SLP-76 regulates ZAP-70 microcluster formation. (*A*) SLP-76 deficient J14 cells show reduced levels of ZAP-70-mRFP clustering relative to SLP-76 positive WT cells. Confocal images of ZAP-70-mRFP cluster formation and distribution at the interface of transfected Jurkat WT or J14 cells and anti-CD3–coated slides (*i*). Jurkat WT cells expressing ZAP-70-mRFP on anti-CD3–coated slides (*Upper Right*) or on control anti-Ig–coated slides (*Upper Left*); SLP-76 deficient J14 cells expressing ZAP-70-mRFP on anti-CD3–coated slides (*Lower Right*) or on control anti-Ig–coated slides (*Lower Left*). (Scale bars, 10 μm.) Histograms showing the number of ZAP-70-mRFP clusters per cell (*ii*), the percentage of cells expressing ZAP-70-mRFP clusters (*iii*) and displacement values of ZAP-70-mRFP clusters in WT (green curve) and J14 (red curve) cells over time as determined by Volocity software (*iv*). Values for motility were calculated by Volocity software from the time-lapse movies. (*B*) Inhibition of ZAP-70-mRFP clustering by coexpression of SLP-76 4KE mutant. Confocal images of ZAP-70-mRFP (red) and SLP-76-EYFP (green) microclustering at the interface between transfected J14 cells and anti-CD3–coated coverslips. J14 cells were cotransfected with ZAP-70-mRFP and SLP-76-EYFP WT (*i*) or ZAP-70-mRFP and SLP-76-EYFP 4KE mutant (*ii*). (*Insets*) The transient interactions between ZAP-70-mRFP microclusters and SLP-76-EYFP WT microclusters in selected regions over 24 s. (Scale bars, 10 μm.) Histograms show cluster sizes of ZAP-70-mRFP and SLP-76-EYFP WT (*iii*), percentage of cells with ZAP-70 clustering in presence of SLP-76 WT or 4KE mutant expression (*iv*) and displacement values of ZAP-70 clusters (red curve) and SLP-76 clusters (green curve) over 175 s (*v*). (*C*) SLP-76 4KE impairs ZAP-70-mRFP cluster formation in human primary T cells. Confocal images of ZAP-70-mRFP (red) and SLP-76-EYFP (green) microclustering at the interface between transfected human primary T cells and anti-CD3–coated coverslips. Human primary T cells were cotransfected with ZAP-70-mRFP and SLP-76-EYFP WT (*i*, *Upper*) or ZAP-70-mRFP and SLP-76-EYFP 4KE mutant (*i*, *Lower*). (Scale bars, 5 μm.) Histograms show cluster size of ZAP-70-mRFP and SLP-76-EYFP (*ii*) and percent of cells with ZAP-70 clusters in SLP-76 and SLP-76 4KE cotransfected cells (*iii*).

mRFP clusters in J14 cells also had limited movement as seen in tracking plots (Fig. S1*Af*), and by the small displacement values (Fig. 1*Aiv*). WT and J14 Jurkat cells bound and underwent similar spreading on the anti-CD3–coated slides. The observations indicated that SLP-76 expression is needed for the optimal formation of ZAP-70 microclusters in response to anti-CD3.

Using a complementary approach, a mutant of SLP-76 where four conserved lysine residues at 259/260 and 303/304 were replaced by glutamic acid (E) (termed 4KE) was assessed for effects on ZAP-70 clustering. SLP-76-EYFP or 4KE-EYFP was coexpressed with ZAP-70-mRFP in J14 cells and imaged at the point of contact with immobilized anti-CD3 on slides (Fig. 1*B*). SLP-76-EYFP and ZAP-70-mRFP underwent extensive clustering in response to anti-CD3 (Fig. 1*Bi*, Movie S2, and Movie S3). The SLP-76 clusters were generally larger than the ZAP-70 clusters (i.e., average size of 2.1 vs. 0.36 μm^2) (Fig. 1*Biii*), and underwent greater movement as seen by the displacement values (green curve, Fig. 1*Bv*). SLP-76-EYFP clusters formed initially in peripheral areas and moved to the center part at the interface, as previously described (21, 22, 30). Further, the clusters intersected reiteratively with approximately 5% of the ZAP-70 clusters interacting with SLP-76 clusters and vice versa at any one time (Fig. 1*B Inset*). By contrast, the 4KE SLP-76 mutant was impaired in cluster formation and blocked the ability of coexpressed ZAP-70-mRFP to form clusters (Fig. 1*Bii* and Fig. S2). Although 32% of SLP-76 reconstituted cells showed ZAP-70-mRFP clustering, less than 3% of 4KE SLP-76 expressing cells showed ZAP-70-mRFP clustering (Fig. 1*Biv*). This occurred under conditions where the 4KE mutant still bound to GADS and ADAP (Fig. S3*A*). Expression of SLP-76 in J14 cells increased phosphorylation of LAT and ZAP-70 in response to anti-CD3 (Fig. S3*B*, lanes 3 and 4 vs. 1 and 2), whereas SLP-76 4KE expression showed a lesser effect than wild type SLP-76 (lanes 5 and 6). In agreement, the reduction in ZAP-70 clustering was accompanied by a reduction in anti-CD3 induced ZAP-70 phosphorylation at activation residues Y-319 and Y-493 as measured by intracellular staining (Fig. S4).

Importantly, 4KE SLP-76 had a similar inhibitory effect on ZAP-70-mRFP clustering in primary human T cells (Fig. 1*Ci Lower* vs. *Upper*). Purified T cells were stimulated for 48 h, transfected, rested overnight, and then imaged on anti-CD3–coated slides. Although 13% of cells coexpressing ZAP-70-mRFP with SLP-76-EYFP WT showed ZAP-70-mRFP clustering, only 3% of cells coexpressing ZAP-70-mRFP with SLP-76-EYFP 4KE mutant showed ZAP-70-mRFP cluster formation (Fig. 1*Ciii*). The mean size of ZAP-70 clusters was smaller than SLP-76-EYFP clusters (i.e., 0.95 vs. 1.6) (Fig. 1*Cii*). Overall, using J14 cells or primary T cells, our findings show that the absence of SLP-76, or the presence of mutant SLP-76 can exert feedback control on ZAP-70 clustering.

Loss of the SLP-76 SH2 Domain Failed to Affect ZAP-70 Clustering. SLP-76 has an SH2 domain that binds to the adaptor ADAP and HPK1 (9–13). Recently, the SH2 domain of SLP-65, the B cell analog of SLP-76, has been reported to bind to ZAP-70 related SYK (31). It was therefore possible that the SLP-76 SH2 domain bound to ZAP-70 and accounted for SLP-76 effects on ZAP-70. To assess this, an inactivating SH2 domain mutation (i.e., R448L) was generated on the WT and 4KE forms of SLP-76 and assessed for effects on ZAP-70-mRFP clustering (Fig. 2*A*). The R448L mutation on WT SLP-76 allowed for normal ZAP-70

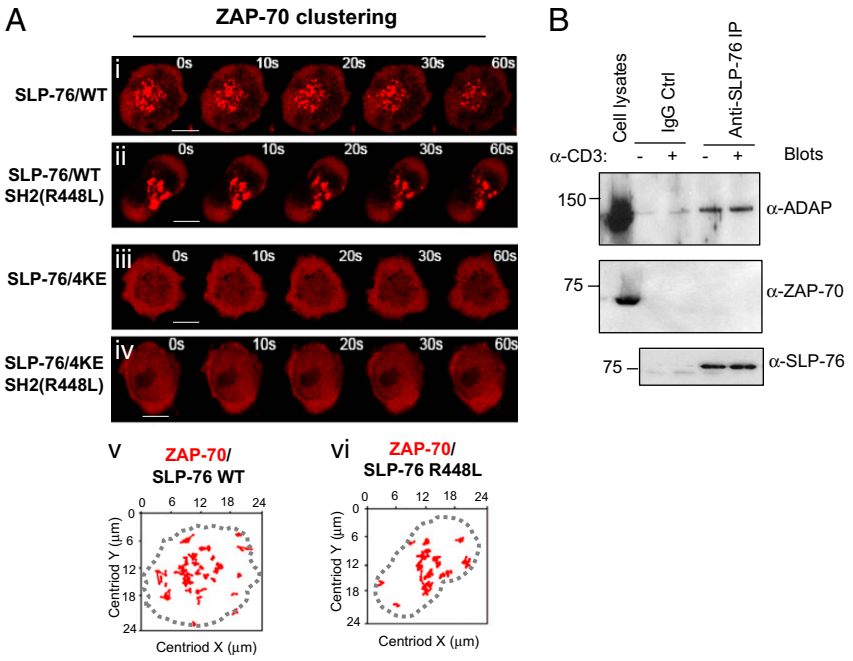

Fig. 2. Putative SLP-76 SH2 domain binding to ZAP-70 is detectable and cannot account for SLP-76 regulation of ZAP-70 clustering (*A*) Inactivation of the SH2 domain in the SLP-76 4KE mutant failed to alter its ability to disrupt ZAP-70 clustering. Time-lapse confocal images of ZAP-70 microclusters formation at the interface between transfected J14 Jurkat T cells and antigenic coverslips. ZAP-70-mRFP was coexpressed in cells with SLP-76 WT (*i*), SLP-76-SH2-(R448L) (*ii*), SLP-76–4KE (*iii*) or in SLP-76–4KE-SH2 (R448L) (*iv*). Panels are representative of at least eight cells. (Scale bars, 10 μm.) The movement of ZAP-70 individual cluster in cells over expressing SLP-76 WT (*v*) or SLP-76 R448L (*vi*) over the time course was tracked. The dotted line indicates boundary of T cell/coverslip interface. (*B*) SLP-76 fails to coprecipitate ZAP-70. SLP-76 was immunoprecipitated by anti-SLP-76 monoclonal antibody from Jurkat cells in the presence or absence of anti-CD3. The immunoprecipitates were subjected to SDS/PAGE, immunoblotted using anti-ADAP (*Top*); anti-ZAP-70 (*Middle*); anti-SLP-76 (*Bottom*).

clustering and the ZAP-70 clusters in R488L SLP-76 expressed cells were at a similar size and even occasionally larger than observed in the presence of WT SLP-76 (Fig. 2*A i*, *ii*, *v*, and *vi*, tracking plots).

Further, the R448L mutation in SLP-76 4KE did not affect mutant disruption of ZAP-70 clustering over 60 s (Fig. 2*Aiv*). Both 4KE and 4KE/R488L inhibited ZAP-70 clustering (i.e., >95% of cells). This was also detected at later times (i.e., 125–300 s). In addition, anti-SLP-76 failed to coprecipitate ZAP-70 from resting and anti-CD3 activated T cells (Fig. 2*B*). As a control, anti-SLP-76 readily coprecipitated ADAP, as previously shown (9–11). The SLP-76 SH2 domain therefore did not show detectable binding to ZAP-70 and, consistent with this, inactivation of the SLP-76 SH2 domain did not alter the inhibitory effect of SLP-76 4KE on ZAP-70 clustering.

SLP-76 4KE Mutant Disrupts GADS Cluster Formation. A similar loss of GADS-mCherry clustering was observed in SLP-76 4KE expressing cells (Fig. 3). SLP-76-EYFP and GADS-mCherry readily clustered in response to anti-CD3 and showed extensive overlap (Fig. 3*A Upper* see *Center Inset*; yellow color, and Movie S4). They also moved with the same speed (i.e., 0.05–0.06 μm/s) (Fig. 3*B*). This close connection in clustering has been previously reported (23) and is consistent with avid GADS SH3 domain binding to SLP-76 (5). By contrast, coexpression of the SLP-76 4KE mutant prevented GADS-mCherry clustering (Fig. 3*A Lower*). These observations confirm that GADS clustering is dependent on SLP-76.

LAT Clustering Occurs Independently of SLP-76. It was next of interest whether LAT clustering was regulated by SLP-76 (Fig. 4). LAT operates upstream with ZAP-70 phosphorylation sites that recruit the GADS-SLP-76 complex (32). Microcluster formation of LAT-mCherry was examined in WT and J14 Jurkat cells (Fig. 4*A*). Intriguingly, LAT-mCherry readily formed microclusters in both cells over a time course (Fig.4*Ai* and Fig. S5*A*). A similar percent of WT and J14 cells showed LAT clusters (Fig. 4*Aii*, gray and red bars), whereas the velocity (i.e., 0.29–0.30 μm/s), displacement, and travel distance of LAT cluster movement were similar in WT and J14 cells (Fig. 4*A iii*, *iv*, and *v*). Moreover, as measured by a second approach, LAT-mCherry cluster formation was also unaffected by the coexpression of SLP-76 4KE (Fig. 4*B i* vs. *ii*, Fig. S5*B*, and Movie S5). SLP-76-EYFP and LAT-mCherry clusters transiently intersected with approximately 10% colocalization at any one point (Fig. 4*B Center Inset*). PCC values confirmed this copositioning with values between 0.35 and 0.47 as averaged over the time course (Fig. 4*Bvi*). By contrast, whereas SLP-76 4KE-EYFP remained mostly diffuse and unclustered, coexpressed LAT-mCherry showed numerous clusters (Fig. 4*Bii*). Although LAT clusters moved more quickly than SLP-76 clusters (i.e., 0.25 vs. 0.1 um/s) (Fig. 4*Biv*), they moved at similar speeds in SLP-76 and SLP-76 4KE transfected cells (Fig. 4*Bv*). Given the absence of SLP-76 4KE clusters, it was difficult to assess their colocalization; however, PCC values for SLP-76 4KE and LAT were reduced (i.e., 0.1–0.25) (Fig. 4*Bvi*, pink curve).

LAT clustering independence from SLP-76 was also seen in human primary T cells expressing the SLP-76 4KE mutant (Fig. 4*Ci* and Movie S6). As in Jurkat cells, a similar percentage of cells showed LAT-mCherry clusters (Fig. 4*Cii*). Further, although LAT-mCherry clusters moved faster than SLP-76-EYFP clusters (0.21 vs. 0.14 μm/s) (Fig. 4*Ciii*), they moved at similar speeds in SLP-76 and SLP-76 4KE transfected cells (Fig. 4*Civ*). These observations clearly showed that unlike in the case of ZAP-70 and GADS, LAT cluster formation is unaffected by the loss of or altered SLP-76.

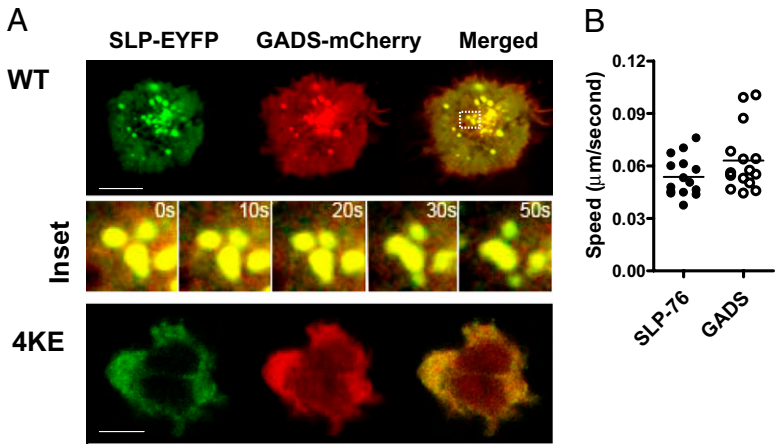

Fig. 3. The SLP-76 4KE mutant disrupts GADS microcluster formation. Confocal images of GADS-mCherry and SLP-76-EYFP cluster formation and distribution at the interface of transfected cells and anti-CD3–coated slides (*A*). Jurkat cells were cotransfected with and GADS-mCherry (red) and SLP-76-EYFP WT (green) (*Upper*) or with GADS-mCherry and SLP-76-EYFP 4KE mutant (*Lower*). (Scale bars, 10 μm.) Insets show time-lapse series of GADS and SLP-76 WT microcluster movement in selected regions imaged over 50 s. Histogram shows the speed (μm/s) traveled by individual clusters over time within cells cotransfected with SLP-76-EYFP WT and GADS-mCherry (*B*).

Discussion

The canonical TCR signaling pathway involves CD4-p56lck recruitment of ZAP-70 to the antigen-receptor followed by ZAP-70 activation and its phosphorylation of SLP-76/LAT followed by LAT binding to the GADS-SLP-76 complex (1–3). Original imaging studies by Bunnell et al. (20, 22, 23) showed that ZAP-70, GADS, and SLP-76 microcluster formation depends on LAT. Others have documented differences in the behavior of SLP-76 and ZAP-70 clustering during the maturation of the IS (8, 23, 30, 33, 34). Despite these important advances, it had been unclear whether the pathway from ZAP-70 to LAT to GADS/SLP-76 is strictly linear or involves additional levels of complexity and feedback regulation. In this study, we have provided evidence that SLP-76 can exert a cross-regulatory or feedback control on the clustering of ZAP-70, an element previously thought to operate exclusively upstream of SLP-76. Using two independent and complementary approaches, we showed that ZAP-70 cluster formation is impaired in J14 Jurkat cells lacking SLP-76 and in Jurkat and human primary T cells expressing the SLP-76 mutant 4KE. The number of cells expressing clusters and the number of clusters per cell were significantly reduced. By contrast, LAT clustering was unaffected. TCR signaling is therefore not a strictly linear series of events but rather involves an additional layer of feedback or cross-regulation of ZAP-70 by SLP-76 (Fig. 4*D*). This feedback mechanism could act to control the level of activation of this key upstream component in the TCR signaling cascade. Proper SLP-76 engagement would be needed before further amplification of ZAP-70 activation would be allowed. Otherwise, a decoupled connection or balance between ZAP-70 and SLP-76 might result in inefficient signaling or the inappropriate engagement of other substrates by the kinase. Overall, feedback or cross-regulatory control might act to fine-tune the TCR response by promoting the balanced integration of signals.

ZAP-70 clustering was reduced in T cells lacking SLP-76 or expressing the SLP-76 4KE mutant (Fig. 1). In J14 cells, the number of cells with clusters and the number of clusters per positive cell was reduced by more than 50%, whereas SLP-76 4KE mutant appeared to have a more potent effect (i.e., >95%) (Fig. 1). The basis for this difference is not clear, although low, marginally detectable levels of SLP-76 can be seen in J14 cells, suggesting that the cell line has greatly reduced SLP-76 rather than being entirely devoid of the adaptor (8). At the same time, we cannot exclude that SLP-76 4KE could act as a dominant negative in its blockade of ZAP-70 clustering. Although the exact basis for the action of the 4KE mutant remains to be elucidated, GADS and ADAP bound normally. Impairment in ZAP-70 clustering was observed at all time points (0-250 s) and in more than 10 separate experiments and is unlikely due to an indirect secondary effect on the efficiency of receptor clustering or adhesion because all of the imaged cells adhered and spread normally on anti-CD3–coated slides. Further, importantly, LAT clustering occurred normally in J14 and SLP-76 4KE expressing cells and therefore served as an excellent positive control (Fig. 4). One strength of our study was the use of two independent and complementary approaches to examine the effect of SLP-76 on ZAP-70 clusters. The use of J14 cells and the 4KE mutant led to the same conclusion, namely in both cases, we observed that alterations in SLP-76 can impair ZAP-70 clustering (Fig. 1). The use of the 4KE mutant further allowed confirmation of effects in human primary T cells. Overall, our findings clearly implicate SLP-76 in the regulation of ZAP-70 cluster formation in T cells without affecting the clustering of LAT.

The underlying molecular basis for the regulatory effect of SLP-76 awaits further investigation and may require a better understanding of the fundamental mechanisms responsible for the formation of signaling clusters. This is presently poorly understood. ZAP-70 recruitment to TCR clusters can be inhibited by inhibition of *src* kinases (i.e., PP2A) (22). An analysis of the various SLP-76 mutants that mediate an effect on ZAP-70 may provide additional clues. In this regard, we made an attempt to assess whether SLP-76 SH2 domain binding to ZAP-70 could account for the effect. A previous study reported that the SH2 domain of SLP-65 bound to ZAP-70 related kinase SYK (31). Despite this, and the fact that ZAP-70 phosphorylates SLP-76 (30), we could find no evidence of binding between SLP-76 and ZAP-70. In repeated experiments, anti-SLP-76 failed to coprecipitate ZAP-70 in response to anti-CD3 ligation, despite coprecipitating ADAP (Fig. 2*B*). Further, inactivation of the SH2 domain (i.e., R488L mutation) on the 4KE background (i.e., 4KE/R488L) blocked ZAP-70 clustering (Fig. 2*A*). The inhibition by 4KE/R488L was as effective as seen with the SLP-76 4KE mutant. Intriguingly, mutation of the R488 site in WT SLP-76 mutant did not cause it to inhibit ZAP-70 clustering. SLP-76 binding to ADAP and HPK1 is therefore not needed for ZAP-70 clustering. Further, SH2 domain mutants fail to cluster (29) and yet supported normal ZAP-70 clustering (Fig. 2), suggesting that SLP-76 cluster formation itself may not be needed for ZAP-70 clustering. The impaired clustering of SLP-76 4KE is therefore

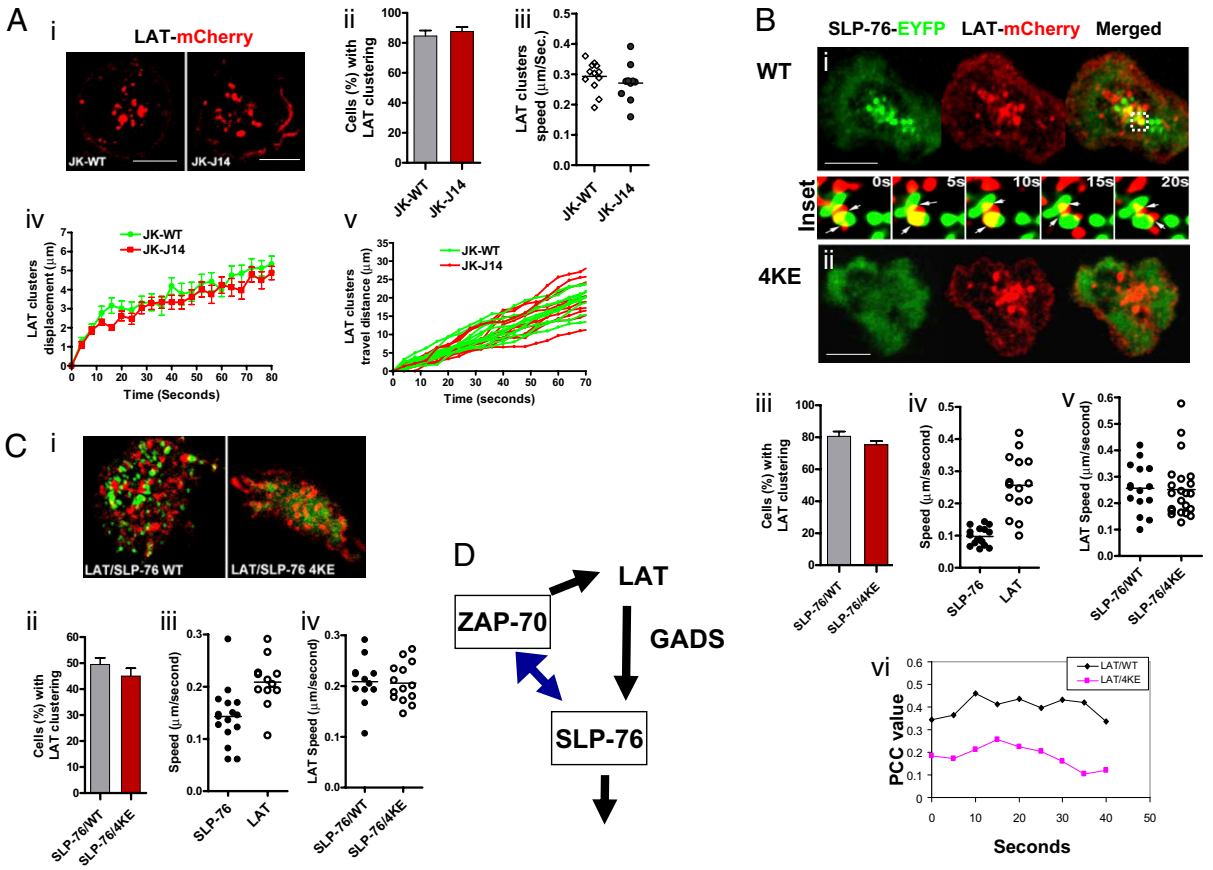

Fig. 4. LAT clustering occurs independently of SLP-76. (*A*) LAT-mCherry clustering in Jurkat WT or SLP-76 deficient J14 cells. Confocal images of LAT-mCherry cluster formation and distribution at the interface of transfected cells and anti-CD3–coated slides (*i*) LAT-mCherry microcluster formation in Jurkat WT cells (*Left*) or in SLP-76 deficient J14 cells (*Right*). (Scale bars, 10 μm.) Histograms show the percentage of cells expressing LAT-mCherry clusters in WT (gray bar) and J14 (red bar) cells (*ii*) values of speed of movement of LAT clusters (*iii*), displacement values of LAT-mCherry clusters (*iv*) and distance traveled over time by individual LAT clusters (*v*) in WT Jurkat cells or J14 cells. Values for motility were calculated by Volocity software from the time-lapse movies. (*B*) LAT clustering in J14 cells cotransfected with SLP-76 WT or 4KE mutant. Confocal images of LAT-mCherry and SLP-76-EYFP cluster formation and distribution at the interface of transfected J14 cells and anti-CD3–coated slides. J14 cells were cotransfected with LAT-mCherry (red) and SLP-76-EYFP WT (green) (*i*) or with LAT-mCherry (red) and SLP-76-EYFP 4KE mutant (*ii*). Insets between *i* and *ii* show the movement and interaction of LAT-mCherry and SLP-76-EYFP clusters in selected regions over 20 s. (Scale bars, 10 μm.) Histograms show the percentage of cells with LAT clusters in Jurkat cells cotransfected with SLP-76-EYFP WT (gray bar) or SLP-76-EYFP 4KE mutant (red bar) (*iii*), the speed (μm/s) traveled by individual SLP-76 versus LAT clusters in cells coexpressed with LAT-mCherry and SLP-76-EYFP WT (*iv*), the speed of LAT clusters in cells cotransfected SLP-76-EYFP WT or 4KE mutant (*v*) and Pearson's correlation coefficient (PCC) values of the overlap of LAT-mCherry and SLP-76-EYFP WT or LAT-mCherry and SLP-76-EYFP 4KE over a time-course (*vi*). Values for motility and PCC were calculated by Volocity software from the time-lapse movies. (*C*) LAT clustering is not affected in primary T cells expressing SLP-76 4KE mutant. Confocal images of LAT-mCherry and SLP-76-EYFP cluster formation and distribution at the interface of transfected human primary T cells and anti-CD3–coated slides (*i*). Human primary T cells were cotransfected with LAT-mCherry (red) and SLP-76-EYFP WT (green) (*Left*) or with LAT-mCherry (red) and SLP-76-EYFP 4KE mutant (green) (*Right*). Histograms show the percentage of cells with LAT clusters in human primary T cells cotransfected with SLP-76-EYFP WT or 4KE mutant (*ii*), the speed (μm/s) traveled by individual SLP-76 versus LAT clusters in cells coexpressed with LAT-mCherry and SLP-76-EYFP WT (*iii*) and the speed of LAT clusters in cells cotransfected SLP-76-EYFP WT or 4KE mutant (*iv*). Values for motility were calculated by Volocity software from the time-lapses movies. (*D*) Feedback regulation of ZAP-70 clustering by SLP-76, whereas LAT clustering is independent. Phosphorylation of LAT is needed to recruit GADS and SLP-76 into the LAT signalosome. Disruption of LAT signaling can interfere with clustering of GADS and LAT. Similarly, disruption of GADS affects SLP-76 clustering. We show that ZAP-70 clustering is partially dependent on SLP-76. LAT to GADS to SLP-76 is therefore not a strictly linear pathway but involves a feedback loop where ZAP-70 and GADS clustering is dependent on SLP-76. By contrast, LAT clustering is unaffected by the loss of SLP-76 clustering.

also unlikely to be responsible for reduced ZAP-70 clustering. Previous studies have shown that SLP-76 clusters form normally in a PLCγ1 deficient cell line (29). Other possible mechanisms of SLP-76 influence on ZAP-70 could include Vav1 or interleukin-2-inducible T cell kinase (ITK) binding to SLP-76 and the cytoskeleton (35–37).

Given the close connection between LAT and SLP-76 in the LAT signalosome, it was intriguing that LAT clustered normally in J14 cells, and in the presence of SLP-76 4KE (Fig. 4). Neither the number, size, nor motility of clusters was altered. A greater number of cells routinely showed more LAT than ZAP-70 clusters in Jurkat and primary T cells, and LAT clusters moved more rapidly than ZAP-70 clusters. The forces that drive LAT transmembrane clustering may therefore be more powerful than the potential regulatory effects of SLP-76. Alternatively, LAT clustering as a transmembrane protein may be regulated by distinct events. LAT clustering is dependent on tyrosine residues (22) such that mutation of the sites impairs its clustering (26, 27). LAT phosphorylation was only marginally decreased despite the lack of ZAP-70 clustering. Unclustered ZAP-70 may therefore retain an ability to phosphorylate LAT and/or kinases such as p56lck may substitute for less efficient ZAP-70 function (38). Similarly, LAT tyrosine phosphorylation has been reported to be unaltered in SLP-76-deficient mice (39). In conclusion, our findings show

that SLP-76 regulates the other cytoplasmic kinase and adaptor ZAP-70 and GADS, whereas upstream transmembrane LAT operates independently in the TCR signaling cascade.

Materials and Methods

Cell Culture and Antibodies. Jurkat T cells (ATCC) and SLP-76 deficient Jurkat J14 (a kind gift from A. Weiss, University of California San Francisco, CA) were maintained in RPMI medium 1640 supplemented with 5% (vol/vol) FCS, 1% (wt/vol) penicillin/streptomycin, and 1% (vol/vol) L-glutamine. Anti-human CD3 (OKT3) were purchased from ATCC. Anti-SLP-76 monoclonal antibody was a kind gift from Paul R. Findell (Syntex, Palo Alto, CA). Anti-ADAP and anti-GADS antibodies were purchased from Upstate Biotechnology. Anti-total ZAP-70 antibody was purchased from Santa Cruz Biotechnology and anti-pTy319 and anti-pTy493 of ZAP-70 antibodies were purchased from Cell Signaling Technology.

Expression Vectors and Plasmids. SLP-76-YFP fusion construct, the human SLP-76 cDNA, was amplified by PCR and was subcloned into the XhoI/BamHI sites of pEYFP-N1 vector (Clontech). The LAT-mCherry and GADS-mCherry fusion constructs were generated by subcloning the RT-PCR amplified cDNAs encoding either protein into the Hind III/BamH I sites and Kpn I/BamH I sites of pcDNA3-mCherry vector, respectively. The 4KE SLP-76 mutant was generated by point mutations of lysine to glutamatic acid using a site-directed mutagenesis kit (QuikChange; Stratagene) with primers: 5′- gaa ccc ttc aca cta gga gag gaa cca cca tttt ctg ac -3′ and 5′- gtgg cac agg tgg ctc ctc ccc tgg cagg-3′. The SLP-76 SH2 domain R448L mutants in pcDNA3.1 were made using the same method with the primers: 5′-Caggatggcacatttctggtcttagacagctctaaaaaaacaacaacc-3′ and 5′-Ggttgttgttttttta gagctg tctaagaccagaaatgtgccatcctg-3′. Peripheral blood lymphocytes were isolated from buffy-coats by density gradient centrifugation (9). Jurkat WT cells and J14 cells were transfected by microporation (Digital Bio Technology), using a single pulse of 30 ms at 1410 V, and the activated human primary T cells were transfected using a single pulse of 20 ms at 2259 V. Intracellular staining with anti-ZAP-70, anti-phospho-Y319 and anti-phospho-493 was conducted as previously described (27, 28).

Confocal Imaging. For live cell imaging, polylysine (Sigma) treated chambered coverslides (LabTek) were coated with 5–15 ug/mL anti-CD3 mAb OKT-3 for 1 h at 37 °C to generate antigenic surfaces as described (22, 23). Cells were imaged by a resonance scanning confocal microscopy (TCS SP5 RS; Leica) using excitation wavelengths of 514 nm (for EYFP), 458 nm (for mCFP), and 594 nm (for mRFP and mCherry) and a 63× water immersion objective (NA = 1.2), or a Zeiss LSM 510 confocal microscopy. Simultaneous imaging of different fluorophores was acquired by sequential line scanning. Images were processed with Leica confocal software (LCS; Leica Microsytems), Volocity (Improvision), and ImageJ (National Institutes of Health) software.

1. Samelson LE (2002) Signal transduction mediated by the T cell antigen receptor: The role of adapter proteins. *Annu Rev Immunol* 20:371–394.
2. Rudd CE (1999) Adaptors and molecular scaffolds in immune cell signaling. *Cell* 96: 5–8.
3. Jordan MS, Singer AL, Koretzky GA (2003) Adaptors as central mediators of signal transduction in immune cells. *Nat Immunol* 4:110–116.
4. Zhang W, Sloan-Lancaster J, Kitchen J, Trible RP, Samelson LE (1998) LAT: The ZAP-70 tyrosine kinase substrate that links T cell receptor to cellular activation. *Cell* 92:83–92.
5. Berry DM, Nash P, Liu SK, Pawson T, McGlade CJ (2002) A high-affinity Arg-X-X-Lys SH3 binding motif confers specificity for the interaction between Gads and SLP-76 in T cell signaling. *Curr Biol* 12:1336–1341.
6. Clements JL, et al. (1998) Requirement for the leukocyte-specific adapter protein SLP-76 for normal T cell development. *Science* 281:416–419.
7. Sommers CL, et al. (2001) Knock-in mutation of the distal four tyrosines of linker for activation of T cells blocks murine T cell development. *J Exp Med* 194:135–142.
8. Yablonski D, Kuhne MR, Kadlecek T, Weiss A (1998) Uncoupling of nonreceptor tyrosine kinases from PLC-gamma1 in an SLP-76-deficient T cell. *Science* 281:413–416.
9. Raab M, Kang H, da Silva A, Zhu X, Rudd CE (1999) FYN-T-FYB-SLP-76 interactions define a T-cell receptor zeta/CD3-mediated tyrosine phosphorylation pathway that up-regulates interleukin 2 transcription in T-cells. *J Biol Chem* 274:21170–21179.
10. da Silva AJ, et al. (1997) Cloning of a novel T-cell protein FYB that binds FYN and SH2-domain-containing leukocyte protein 76 and modulates interleukin 2 production. *Proc Natl Acad Sci USA* 94:7493–7498.
11. Musci MA, et al. (1997) Molecular cloning of SLAP-130, an SLP-76-associated substrate of the T cell antigen receptor-stimulated protein tyrosine kinases. *J Biol Chem* 272: 11674–11677.
12. Di Bartolo V, et al. (2007) A novel pathway down-modulating T cell activation involves HPK-1-dependent recruitment of 14-3-3 proteins on SLP-76. *J Exp Med* 204:681–691.
13. Shui JW, et al. (2007) Hematopoietic progenitor kinase 1 negatively regulates T cell receptor signaling and T cell-mediated immune responses. *Nat Immunol* 8:84–91.
14. Wang H, et al. (2003) SKAP-55 regulates integrin adhesion and formation of T cell-APC conjugates. *Nat Immunol* 4:366–374.
15. Wang H, Rudd CE (2008) SKAP-55, SKAP-55-related and ADAP adaptors modulate integrin-mediated immune-cell adhesion. *Trends Cell Biol* 18:486–493.
16. Davis DM, Dustin ML (2004) What is the importance of the immunological synapse? *Trends Immunol* 25:323–327.
17. Saito T, Yokosuka T (2006) Immunological synapse and microclusters: The site for recognition and activation of T cells. *Curr Opin Immunol* 18:305–313.
18. Houtman JC, Barda-Saad M, Samelson LE (2005) Examining multiprotein signaling complexes from all angles. *FEBS J* 272:5426–5435.
19. Kupfer A, Kupfer H (2003) Imaging immune cell interactions and functions: SMACs and the Immunological Synapse. *Semin Immunol* 15:295–300.
20. Bunnell SC, Kapoor V, Trible RP, Zhang W, Samelson LE (2001) Dynamic actin polymerization drives T cell receptor-induced spreading: A role for the signal transduction adaptor LAT. *Immunity* 14:315–329.
21. Yokosuka T, et al. (2005) Newly generated T cell receptor microclusters initiate and sustain T cell activation by recruitment of Zap70 and SLP-76. *Nat Immunol* 6: 1253–1262.
22. Bunnell SC, et al. (2006) Persistence of cooperatively stabilized signaling clusters drives T-cell activation. *Mol Cell Biol* 26:7155–7166.
23. Bunnell SC, et al. (2002) T cell receptor ligation induces the formation of dynamically regulated signaling assemblies. *J Cell Biol* 158:1263–1275.
24. Monks CR, Freiberg BA, Kupfer H, Sciaky N, Kupfer A (1998) Three-dimensional segregation of supramolecular activation clusters in T cells. *Nature* 395:82–86.
25. Dustin ML (2005) A dynamic view of the immunological synapse. *Semin Immunol* 17: 400–410.
26. Huse M, et al. (2007) Spatial and temporal dynamics of T cell receptor signaling with a photoactivatable agonist. *Immunity* 27:76–88.
27. Wang H, et al. (2004) ADAP-SLP-76 binding differentially regulates supramolecular activation cluster (SMAC) formation relative to T cell-APC conjugation. *J Exp Med* 200: 1063–1074.
28. Schneider H, Smith X, Liu H, Bismuth G, Rudd CE (2008) CTLA-4 disrupts ZAP70 microcluster formation with reduced T cell/APC dwell times and calcium mobilization. *Eur J Immunol* 38:40–47.
29. Nguyen K, Sylvain NR, Bunnell SC (2008) T cell costimulation via the integrin VLA-4 inhibits the actin-dependent centralization of signaling microclusters containing the adaptor SLP-76. *Immunity* 28:810–821.
30. Varma R, Campi G, Yokosuka T, Saito T, Dustin ML (2006) T cell receptor-proximal signals are sustained in peripheral microclusters and terminated in the central supramolecular activation cluster. *Immunity* 25:117–127.
31. Kulathu Y, Hobeika E, Turchinovich G, Reth M (2008) The kinase Syk as an adaptor controlling sustained calcium signalling and B-cell development. *EMBO J* 27: 1333–1344.
32. Cho S, et al. (2004) Structural basis for differential recognition of tyrosine-phosphorylated sites in the linker for activation of T cells (LAT) by the adaptor Gads. *EMBO J* 23:1441–1451.
33. Yablonski D, Weiss A (2001) Mechanisms of signaling by the hematopoietic-specific adaptor proteins, SLP-76 and LAT and their B cell counterpart, BLNK/SLP-65. *Adv Immunol* 79:93–128.
34. Kupfer A (2006) Signaling in the immunological synapse: Defining the optimal size. *Immunity* 25:11–13.
35. Wu J, Motto DG, Koretzky GA, Weiss A (1996) Vav and SLP-76 interact and functionally cooperate in IL-2 gene activation. *Immunity* 4:593–602.
36. Raab M, da Silva AJ, Findell PR, Rudd CE (1997) Regulation of Vav-SLP-76 binding by ZAP-70 and its relevance to TCR zeta/CD3 induction of interleukin-2. *Immunity* 6: 155–164.
37. Berg LJ, Finkelstein LD, Lucas JA, Schwartzberg PL (2005) Tec family kinases in T lymphocyte development and function. *Annu Rev Immunol* 23:549–600.
38. Jiang Y, Cheng H (2007) Evidence of LAT as a dual substrate for Lck and Syk in T lymphocytes. *Leuk Res* 31:541–545.
39. Pasquet JM, et al. (1999) LAT is required for tyrosine phosphorylation of phospholipase cgamma2 and platelet activation by the collagen receptor GPVI. *Mol Cell Biol* 19:8326–8334.